agronomy

MDPI

Article

Moving toward the Biophysical Characterization of the Mangrove Swamp Rice Production System in Guinea Bissau: Exploring Tools to Improve Soil- and Water-Use Efficiencies

Gabriel Garbanzo [1,2,3,*], Jesus Céspedes [1], Joseph Sandoval [2], Marina Temudo [1], Paula Paredes [4] and Maria do Rosário Cameira [4,*]

[1] Forest Research Center (CEF), Instituto Superior de Agronomia, Universidade de Lisboa, Tapada da Ajuda, 1349-017 Lisboa, Portugal; jesusc461@gmail.com (J.C.); marinatemudo@gmail.com (M.T.)
[2] Water Resource Management, Department of Environmental Sciences, Wageningen University & Research, P.O. Box 47, 6700 AA Wageningen, The Netherlands; joseph.sandoval@wur.nl
[3] Agronomic Research Center, School of Agriculture, University of Costa Rica, San José 11501-2060, Costa Rica
[4] LEAF—Linking Landscape, Environment, Agriculture and Food—Research Center, Instituto Superior de Agronomia, Universidade de Lisboa, Tapada da Ajuda, 1349-017 Lisboa, Portugal; pparedes@isa.ulisboa.pt
* Correspondence: juan.garbanzo@ucr.ac.cr (G.G.); roscameira@isa.ulisboa.pt (M.d.R.C.)

Abstract: The mangrove swamp rice production system (MSRPS) in West Africa faces significant challenges in soil, water, and salinity management, making rice production highly vulnerable to variations in the spatio-temporal distribution patterns of rainfall, which are exacerbated by climate change. This study's results can provide the initial basis for co-developing strategies with farmers aiming to contribute to the biophysical characterization of the MSRPS, in particular: (i) estimate the water-harvesting efficiency (WL_{ef}) of the plots in the north and south of Guinea Bissau (GB); (ii) characterize the unevenness of the bottom of the plots, which leads to salinization spots; and (iii) create soil consistency maps to provide farmers with a tool to prioritize sites with optimal conditions for tillage. The research was conducted between 2021 and 2023 in the study site of Cafine-Cafal in the south and Elalab in the north of GB. Systematic soil sampling in a grid was designed to quantify the soil consistency and plot/ridge areas were determined. Linear models were developed to predict biophysical parameters (e.g., effective planting areas and water-logging depths) and geostatistics were used to create soil consistency maps for each study site. The results show precipitation water-harvesting efficiencies of 15% and 16% for the southern and northern regions, respectively. Furthermore, the plasticity limits of 18.6% for Elalab and 35.5% for Cafine-Cafal show the most appropriate times to start tillage in specific areas of the paddies. This study provides information on the efficient management of tillage and freshwater conservation, providing MSRPS farmers with useful tools to counteract the effects caused by salinity and rainfall variability.

Keywords: water management; water harvesting; soil consistency; soil salinity; soil tillage; West Africa

Citation: Garbanzo, G.; Céspedes, J.; Sandoval, J.; Temudo, M.; Paredes, P.; Cameira, M.d.R. Moving toward the Biophysical Characterization of the Mangrove Swamp Rice Production System in Guinea Bissau: Exploring Tools to Improve Soil- and Water-Use Efficiencies. *Agronomy* **2024**, *14*, 335. https://doi.org/10.3390/agronomy14020335

Academic Editor: Bo Zhu

Received: 29 December 2023
Revised: 26 January 2024
Accepted: 2 February 2024
Published: 6 February 2024

1. Introduction

Rice is one of the main cereals in the diet of tropical countries worldwide. According to estimates by the Food and Agriculture Organization, its production has increased from 426 to 510 million tons over the last 10 years [1–3].

In the tropical region of northwest Africa, rice is the most consumed cereal at a regional level, particularly in countries such as Senegal, Guinea Bissau, Guinea Conakry, and The Gambia [4]. These countries have a specific rice production system linked to the mangrove forests of the coastal areas, designated as mangrove swamp rice production systems (MSRPSs).

An MSRPS results from the slashing of the mangrove trees and the construction of dikes for the creation of paddies [5]. Thus, MSRPSs have been pointed out as the main cause of mangrove deforestation in Guinea Bissau [6,7]. Among the West African countries practicing mangrove swamp rice cultivation, Guinea Bissau has the largest area occupied by this farming system [7–9] and the highest total production. This distinctive agro-fishing livestock farming system is based on the development of expertise (for dike and dam construction and maintenance, water management, control of soil fertility and toxicity, and selection of rice varieties) and the intensive mobilization of labor (e.g., for land clearing of mangroves, the construction of dikes and canals, soil desalination, and plowing) at certain periods of the crop cycle [8,10–13]. Both the construction of dikes and bunds that delimit the plot and soil tillage are undertaken manually using a long iron-tipped wooden plow.

Rainfall is the only source of water to meet crop water needs and to flush salt from the soil profile [9,14–16]. Therefore, rice is grown during the rainy season (July to November) when the planting sites become suitable for the rice plant, namely, the salinity has reduced to tolerable levels for rice varieties [14,17]. This makes plant growth difficult [5,18,19] and leads to a large variability in rice productivity across the country. However, the rainfall impact depends on both its annual value and its distribution [20,21]. Climate change and poor water management have led to desertification and the abandonment of many fields, which have become infertile and have high salt concentrations [22–24].

Very few field studies on soil characterization and water management have been carried out on the MSRPS [25,26]. These soils have very particular physical and chemical properties because, as stated above, they were previously occupied by mangroves and flooded with brackish water. Furthermore, the water management of an MSRPS is mainly based on the accumulation of rainwater [18,27].

The dimensions of plots are of great importance as they facilitate the harvesting of fresh water from rainfall, which is crucial for plowing, salt leaching, cation solubility, and optimal rice growth [13]. The dimensions of the plots observed in one region should not be extrapolated to the national level, as there are different cultural practices and knowledge gaps regarding soil, water, and salt management. For example, in years and regions with limited rainfall [20], farmers face the challenge of accumulating enough fresh water to manage their plots. Additionally, as farmers explore new cultivation areas, they change the size of the plots, resulting in increased variability. Therefore, to ensure optimal soil and water management and effective salinity control, it is essential to have a detailed understanding of the plot dimensions at local and regional scales, rather than making generalized assumptions without empirical basis [28]. Although MSRPSs are dominant in coastal areas of Guinea Bissau and Senegal (Casamance) [10,29], there is still a lack of comprehensive information on the specific regional dimensions of these structures.

The biophysical characterization of the MSRPS is an urgent need, with the aim to improve rice production, as suggested in the companion article Garbanzo et al. [30]. This involves studying its physical, biological, and chemical components to understand how they interact in a particular environment. Thus, this approach examines various elements, such as soil properties, climate, water availability, plant genetics, biodiversity, and land-management practices [31–34]. The biophysical characterization of the MSRPS serves as a strategic approach to implementing development interventions from multiple perspectives with the goal of establishing a sustainable and productive system. The development of cropping diagnostic tools for efficient water and soil management represents the first step toward improving rice production [35,36]. The national characterization of MSRPS in Guinea Bissau can provide insights into the different ways in which they can become better adapted to local agroecological conditions in times of climate change [37,38]. Additionally, the development of geospatial distribution maps [39] for specific soil management variables could be helpful in scheduling manual soil preparation tasks. This could promote a more systematic approach to agriculture and rice production that is adapted to the micro-climatic diversity of the country [40]. Therefore, characterizing parameters such as the techniques used in the construction of plots and dams and the soil physical parameters could provide an effective strategy for adapting to climate change by improving water harvesting, reducing rainfall needs, and mitigating desertification in the coastal villages of Guinea Bissau.

Soil consistency limits play an important role in soil tillage, i.e., the preparation of the soil for growing crops. It determines the workability of the soil, and farmers' knowledge of it allows them to understand how easily the soil can be manipulated, shaped, and cultivated [41]. It helps in deciding the right time to till the soil [42–44]. This can also prevent soil compaction, as working beyond the plastic limit can change the soil structure, making it more susceptible to compaction, and reducing the porosity, which has a negative impact on root growth and water infiltration [45–48]. Proper understanding and management of soil consistency limits contribute to the creation of an ideal seedbed. This facilitates seed germination, root growth, and overall plant development. Essentially, knowledge of soil consistency limits enables more informed decisions regarding the timing, depth, and intensity of tillage operations, ultimately contributing to improved soil quality and better crop yields. Soil consistency limits refer to the different moisture contents at which the soil behaves differently [49].

Based on the relationships described above and the research gaps identified in the literature (e.g., [11] and the companion paper Garbanzo et al. [30]), the present study aimed to contribute to the biophysical characterization of the MSRPS in the north and south of Guinea Bissau in order to improve the understanding of the soil–water–salinity relationship for optimized plot management. Specifically, our aim was to (i) estimate the water harvesting efficiency of the plots in the north and south of Guinea Bissau; (ii) characterize the unevenness of the bottom of the plots, which leads to salinization spots; and (iii) create soil consistency maps to provide farmers with a tool to prioritize sites with optimal conditions for tillage.

2. Materials and Methods

2.1. Location and Main Characteristics of the Study Sites

The research presented in this paper was conducted between 2021 and 2023 in two regions of Guinea Bissau (GB). Located in West Africa, GB covers an area of approximately 36,125 km^2 and is bordered by Senegal to the north, and Guinea Conakry to the east and south (Figure 1). Two case studies were selected, one in each region. The Elalab case study was located at 12°14′48.5″ N, 16°26′30.3″ W in the S. Domingos administrative sub-region of Cacheu, which is representative of the "Diola" and "Baiote" ethnic groups' techniques. The Cafine-Cafal case study was located at 11°12′40.4″ N, 15°10′26.7″ W in the Tombali region, which is representative of the "Balanta" ethnic group techniques (Figure 1). Both sites present elevations from zero to two meters above sea level.

According to the Koppen climate classification [50], the climate in these regions is AW, which is a tropical monsoon climate with heavy rainfall during the wet season, which usually lasts from June to October. The coastal zone presents an average annual rainfall between 1500 and 2500 mm [20] and annual average temperatures range from 24 °C to 27 °C [51]. The temperature regime is characterized by a low annual variation, with May being the hottest month (29 °C) and January the coldest one (25 °C) [20].

The agroecosystem has been classified as a rainfed wetland rice ecosystem, particularly within the sub-ecosystems prone to drought and flooding [52]. These are characterized by high salt concentrations, which limits rice cultivation to periods when freshwater storage conditions allow for plant growth. In our case studies, samples were collected and observations were made on the entire mangrove swamp rice area (paddies), particularly the associated mangroves ("bolanha doce") and tidal mangroves ("bolanha salgada"). There are two traditional systems of rice swamp cultivation in GB the inland freshwater swamp fields ("bolanha doce") and mangrove swamp ("bolanha salgada"). Both systems refer to rainfed rice cultivated with a permanent depth of water (permanently flooded paddies) until or almost until the end of the rice cycle. The freshwater swamps ("bolanha doce") where rice is cultivated are located in inland valleys where there is a shallow water table or an impermeable soil layer that allows for water storage, and thus, assures fresh-water harvest. Differently, mangrove swamp rice ("bolanha salgada") is characterized by the former presence of mangrove forests invaded by the tides over the years in a fraction of or the whole area of the rice fields, thus leading to a high concentration of salts in the soils, as described in the companion paper Garbanzo et al. [30].

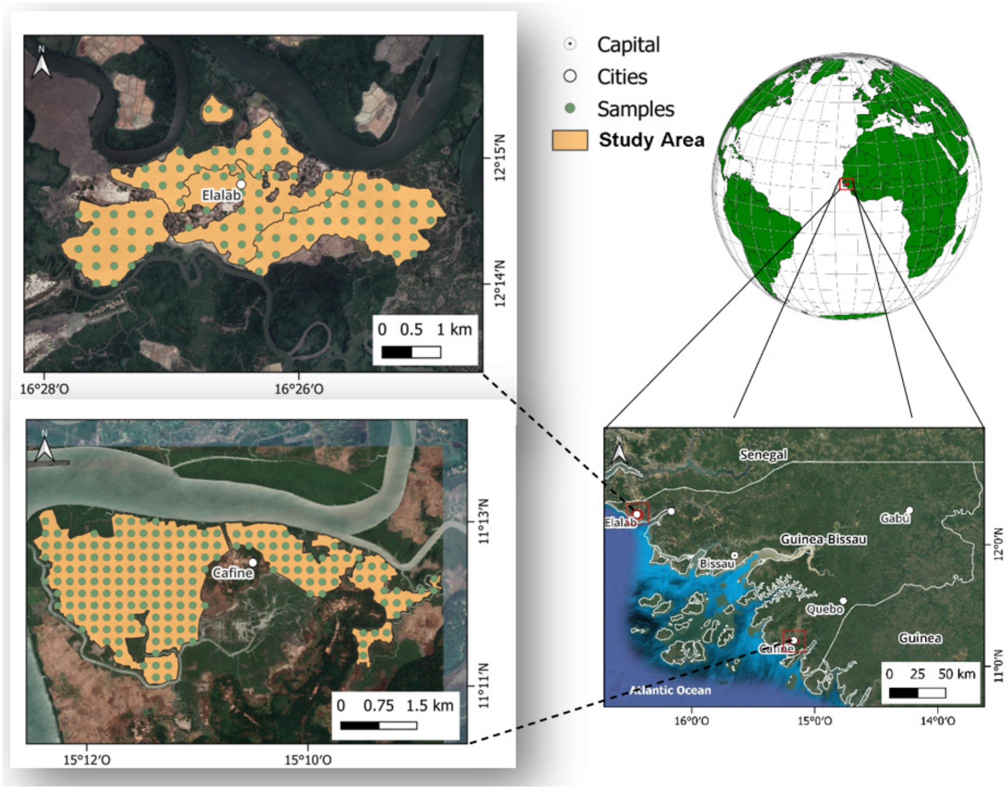

Figure 1. Locations of Guinea Bissau and the study sites Elalab and Cafine-Cafal in the north (S. Domingos, Cacheu) and south (Tombali) of the country, respectively. The maps show points representing the locations where soil samples were taken for physical and chemical analysis.

The soils in the MSRPS areas were included in the orders of the Inceptisols and Entisols according to the Soil Taxonomy–USDA [53]. These soils were formed by alluvial fans that resulted from tidal sedimentations [54–57]. They present a Ustic moisture regime, as they are dry for at least 90 cumulative days in a normal year [55]. Originally, they were mangrove soils that were converted into rice production fields through anthropogenic activities after three to five years of preventing seawater intrusion by building dikes around the planting sites.

2.2. Experimental Observations and Data Collection

Using geographical information system software (QGIS version 3.28.11), polygons were generated to define the rice production areas in Cafine-Cafal and Elalab. Transects were used to assess plots and to delimit the main dikes of the paddies. Once the geographic coordinates of the site were determined, polygons were generated for delimiting the paddies ("Bolanhas") used for cultivation. Google satellite images were used to identify plots and accurately delineate the bunds, enabling the determination of their respective areas. These images were chosen randomly to provide comprehensive coverage of different paddy sites, with a meticulous recording of 100 observations (images) for each study site. Figure 2 shows an image obtained by a drone, illustrating the identification of plots within specific paddy sites, along with the delineation of ridges, furrows, and bunds utilized for rice production.

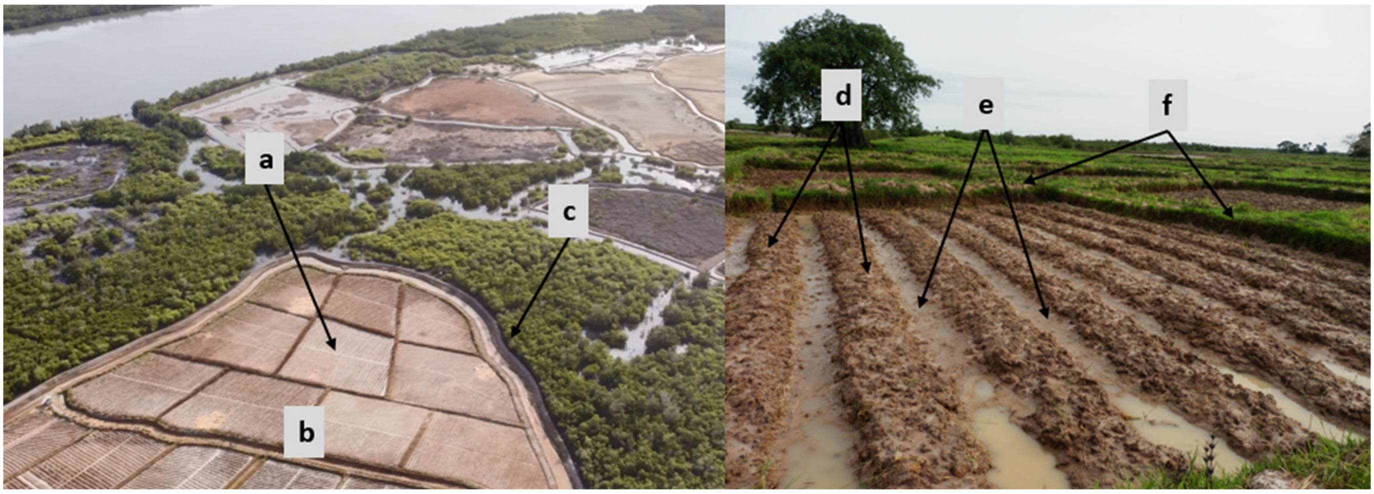

Figure 2. Plots in Mangrove swamp rice in Elalab, Guinea Bissau. Identification of (a) plots, (b) paddies or "Bolanhas", (c) main dikes, (d) ridges, (e) furrows, and (f) bunds.

In order to generate a systematic sampling within a combined area of 1435 ha, a grid of 183 sampling points in Cafine-Cafal and 99 sampling points in Elalab was added to the maps of the rice production areas (Figure 1). The "Cartodroit" application (version V0.61.2_10166) created by the "Instituto Técnico Agrario de Castilla de León" was used for this purpose, as it works in areas without an internet connection. Vector raster layers were generated in Sqlite format to locate the points within the rice production zones. The sampling points were uploaded to a GPS-equipped Android smartphone to precisely identify and locate points within the fields.

Soil samples (282) were collected at each grid point using an auger and shovel at a depth of 0 to 25 cm. The samples were placed in plastic bags and labeled for identification for further processing at the Soil and Water Laboratory of the Ministry of Agriculture and Rural Development of Guinea Bissau. The soil consistency analyses were conducted in Guinea Bissau, whereas the soil chemical analyses (Na, Ca, Mg, K, Al, Fe, pH, electrical conductivity (EC), and exchangeable acidity) were performed at the Soil and Foliar Laboratory of the Agronomic Research Center, University of Costa Rica.

Several measurements were taken in 60 randomly selected plots at each study site during the soil preparation phase (July and August) in order to characterize: (i) the area of the plots, (ii) the area exposed for rice cultivation (ridges), and (iii) the topography of the bottom of the plots.

The sizes of the ridges and the areas of the plots were evaluated in both study sites. The perimeters of the plots were measured with a scale-meter and the areas were quantified. Additionally, the dimensions of three ridges within each plot were measured to quantify the area exposed for rice planting.

The uniformity of plot depths was assessed during the months with the highest rainfall (August to September). The depths were determined by measuring the depth of water inside the plot (waterlogging height) at different points (Figure 3) using a vertical scale meter, yielding 180 measurements for each study site.

Meteorological data was collected during the experimental years in two automatics meteorological stations (ATMOS-41 and ZL6 datalogger): one in the Cafine-Cafal study site (11°13′0.588″ N, 15°10′32.358″ W) and the other in Elalab (12°14′47.54″ N, 16°26′36.424″ W). Data included precipitation, maximum, and minimum temperature.

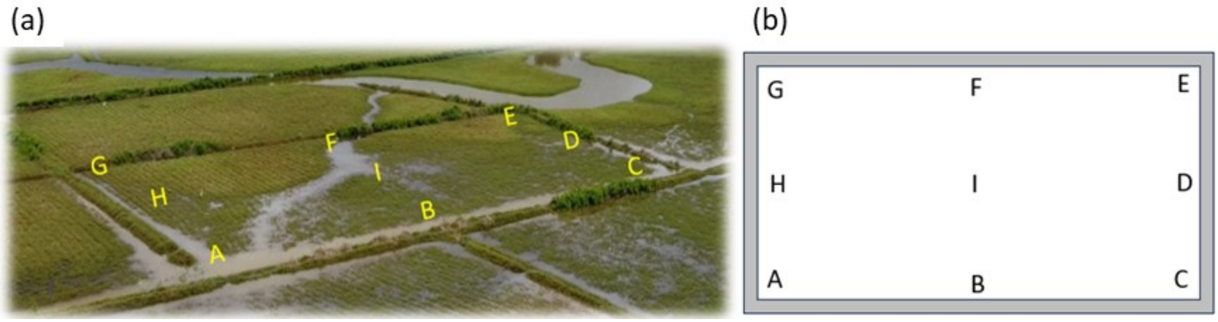

Figure 3. Designated location for measuring the water depth within the plot. (**a**) Drone photo of a plot in Cafine-Cafal and plot-measuring position. (**b**) Conceptual diagram of measuring position.

2.3. Data Treatment

2.3.1. Water Harvesting Efficiency

The water-harvesting efficiency (WL_{ef}) was calculated (Equation (1)) based on the total rainfall recorded during the 2021 and 2022 rainy seasons, as well as the plot dimensions.

$$WL_{ef} = \frac{pa \times pn \times tr}{wl \times pa \times pn} \times 100 \quad (1)$$

where WL_{ef} is the water harvesting efficiency of the plot (%), *pa* is the plot area (m^2), *pn* is the number of "plots numbers per ha" (n), *tr* is the annual rainfall (m m^{-2} $year^{-1}$), and *wl* is the waterlogging height (m).

2.3.2. Soil Consistency and Chemical Analysis

The soil consistency was evaluated using the commonly known methodologies for identifying the Atterberg limits [46,58–60]. For soil consistency determinations, soil samples were air-dried for one month, and sub-samples of 150 g were prepared to determine three consistency limits: the liquid limit (LL), which is the moisture content at which soil transitions from a plastic state to a liquid state (becomes semifluid); the sticky limit (SL), which represents the soil moisture at which the soil no longer adheres to a steel spatula; and the plastic limit (PL), which is the minimum moisture content at which soil remains moldable.

In order to quantify the soil consistency limits, each sample was individually processed as follows: first, the plastic limit (PL) was estimated using the "thread rolling test" in which a square ceramic plate was used to form a 3 mm thread. Second, 50 g of soil was mixed with water until a paste was formed, and then the adhesion was tested with a spatula in order to obtain the sticky limit (SL) [49]. The liquid limit (LL) was then determined using the long-validated methodology developed by Cassagrande [44,46,58–62]. Finally, the gravimetric moisture content was determined in subsamples collected for each consistency limit.

Soil chemical analysis was carried out using extractions with ammonium acetate for Na, Ca, Mg, and K and with ammonium oxalate for Al and Fe. The extractions were analyzed using inductively coupled plasma mass spectrometry to quantify the concentration of elements in each soil sample. In addition, the pH (water), the EC (1:2), and the soil exchangeable acidity were determined. Each soil analysis was conducted in accordance with the Soil Survey Staff methodology [63].

2.3.3. Statistical Data Analysis

The collected data were analyzed separately for each study site. Linear regression analysis (Equation (2)) was used to analyze the correlations between the variables total plot area, rice planting areas on ridges, number of rice production plots, and paddies area. A box plot was also created to analyze the soil consistency results. In addition, analysis of variance and multiple comparisons using Tukey's test ($\alpha = 0.05$) were performed to determine statistical differences between soil consistency results. To perform the above procedures, the RStudio Sofware version 1.4.1103, 2021 [64], was used.

$$y_i = \beta 0 + \beta 1 \chi_i + e_i \quad (2)$$

where y_i is the estimated response (rice planting area on ridges (m^2), number of rice production plots (n)), $\beta 0$ is the estimated intercept in the regression, $\beta 1$ is the estimated slope in the regression, χ_i is the independent variable (total plot area (m^2), area (ha)), and e_i represents the residual error.

A geostatistical analysis was performed using the Geostatistics for Environmental Science (GS+) program. First, the semi-variograms of the soil consistency distributions were analyzed, and the best-fitting model was estimated. Second, the best-fitting models for the Z variables (soil consistency parameters) were created, which were then interpolated using the ordinary Kriging method. Third, the geostatistical analysis tool was used to perform cross-validation through resampling methods (leave-one-out cross-validation "LOOCV") on the previously interpolated information. Fourth, residual errors "e_i" calculated for each observation point were extracted and subtracted from the original value of each observation point to obtain the predictive capacity of each process. Fifth, another geostatistical cross-validation (holdout method "HM") was carried out using 80% of the data to calibrate the models and the other 20% of the data to validate the model as an interpolation result. This process involved removing one data point from the original group and predicting the value of the variable at the location of the removed data point. Subsequently, the root-mean-square error (RMSE), mean absolute error (MAE), and Pearson's correlation coefficient (ρ) were computed to validate the models according to the recommended methodology [65–69]. Finally, the calculated parameters were evaluated using spatial autocorrelation, which was determined using the "Global Mogan's I" statistic, the Z-score, and P-value calculations for each soil consistency parameter (Table 1). The interpolation procedures were performed using the ArcMap 10.8.2 Geostatistical Software and RStudio version 2023.09.1 Build 494 [64].

Table 1. Geostatistical parameters used to calculate the interpolation of soil consistency limits in Cafine-Cafal and Elalab study regions in Guinea Bissau.

Samples	Model	Nugget	Sill	Range
Cafine-Cafal map interpolation			(m)	
SL *	Exponential	22.1	44.2	3192
LL	Exponential	78.0	156.1	1515
PL	Spheric	27.7	73.7	8110
Elalab map interpolation			(m)	
SL	Linear	158.7	158.7	1470.7
LL	Linear	466.9	466.9	1470.7
PL	Linear	47.72	47.72	1470.7

* SL—sticky limit; LL—liquid limit; PL—plastic limit.

3. Results

3.1. Precipitation and Temperature

Figure 4 shows the meteorological data collected from both study sites from 2021 to 2023. Less rainfall was reported at the Elalab study site compared with the Cafine-Cafal site. The sites presented annual rainfalls of 1119–1749 mm and 2476–2679 mm, respectively. The months with the highest rainfall in both years were July, August, and September. The temperature ranged from 22 to 32 °C for both sites. In March and April, there were greater fluctuations between the maximum and minimum temperatures at both sites.

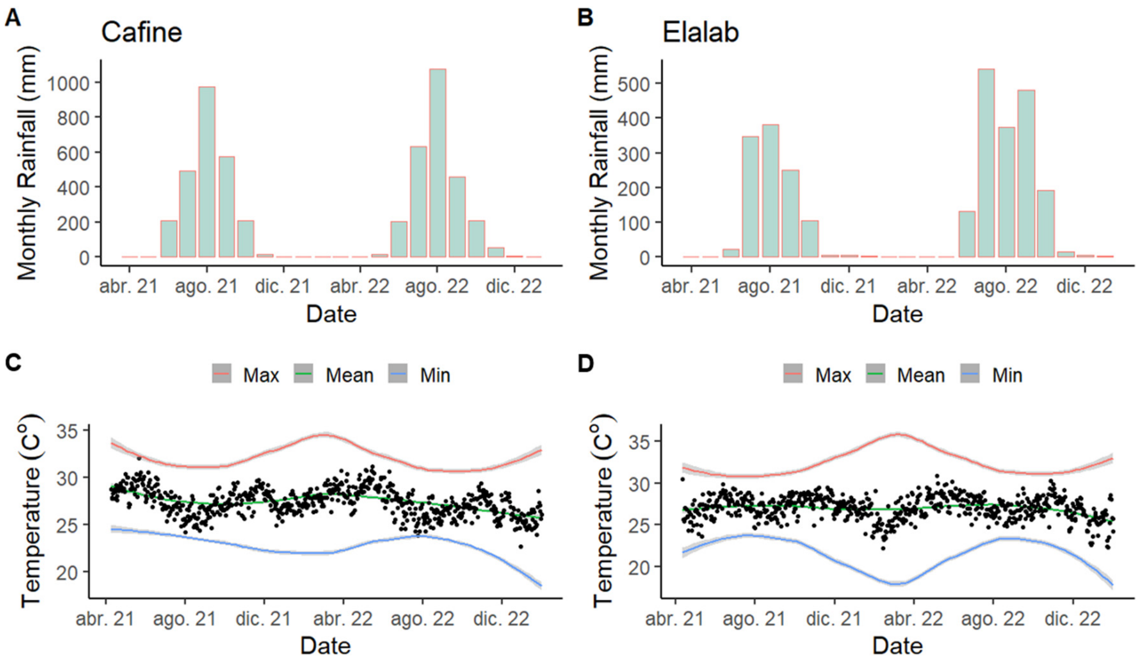

Figure 4. Rainfall and temperatures for Cafine-Cafal (**A**,**C**) and Elalab (**B**,**D**) case study sites from April 2021 to January 2023. The black dots represent the daily average temperature, while the lines illustrate the smoothed curve for maximum, minimum, and average temperatures.

3.2. Soil Chemical Properties

The chemical concentration of nutrients in the areas showed considerable variability (Table 2). The coefficient of variation ranged from 47% to 200% for the Ca, Mg, K, Na, Al, and Fe concentrations. The soils exhibited a pH above 4.4. The Cafine-Cafal soils may present problems associated with exchangeable acidity (>0.5 cmol(+) kg^{-1}), which can affect nutrient availability, hinder root growth, and impact the overall health of crops [70,71]. Furthermore, the average cation-exchange capacity (CEC) was 8.98 cmol(+) kg^{-1} in Elalab and 24.88 cmol(+) kg^{-1} in Cafine-Cafal, with values of Na between 0.11 and 234.96 cmol(+) kg^{-1}. The latter is a substantial amount of sodium, potentially indicating the need for soil amendments or management practices to ensure good conditions for plant growth [71–73]. The notable percentage of saturation bases (SB) indicates high cation concentrations (>175.7%), which may be due to a high sodium concentration in some sites and a low CEC.

Table 2. Soil chemical analysis results for the Elalab and Cafine-Cafal study sites, as measured from samples collected at the beginning of the rainy season between May and June 2021 and 2022.

Site	Statistic	pH	Exchangeable Acidity	Ca	Mg	K	Na	CEC *	SB *	Al	Fe
		H_2O	(KCl 1M)	Extractable NH_4OAC (pH 7.0)						$(NH_4)_2C_2O_4$	
			cmol(+)/kg							%	
Elalab n = 99	Mean	5.9	0.18	3.68	13.66	2.49	75.72	8.98	1566.69	0.04	0.22
	Median	6.0	0.10	2.89	10.77	1.96	59.10	7.02	813.04	0.03	0.16
	Min	3.7	0.07	0.50	0.17	0.02	0.11	0.510	54.08	0.008	0.02
	Max	7.8	2.50	16.89	16.89	9.84	429.00	31.72	13629.21	0.12	1.10
	Std. dev	1.13	0.28	3.29	11.89	2.38	79.32	7.58	2190.83	0.027	0.22
	Coef. var	0.19	1.59	0.89	0.87	0.96	0.99	0.84	1.39	0.77	1.00
Cafine-Cafal n = 183	Mean	4.4	1.12	3.51	12.99	1.95	25.75	24.88	175.68	0.31	0.86
	Median	4.2	0.62	3.19	12.47	1.58	16.49	25.46	130.28	0.11	0.74
	Min	3.2	0.07	0.45	0.09	0.04	0.10	9.25	3.72	0.04	0.13
	Max	7.7	10.90	11.43	33.57	52.96	234.96	42.07	1096.83	5.65	14.71
	Std. dev	0.60	1.38	1.72	6.05	3.92	31.8	4.14	152.49	0.65	1.09
	Coef. var	0.14	1.24	0.49	0.47	2.00	1.24	0.17	0.87	2.13	1.26

* CECN—cation exchange capacity [74]; SBN—percent base saturation ({[Ca + Mg + K + Na]/CEC} × 100).

3.3. Effective Planting Areas and Number of Plots

Figure 5 shows the effective planting area (planting area of the ridges) as a function of the plot areas. The total ridge area was 9.5% greater in the northern study sites (Elalab study site) compared with the southern ones (Cafine-Cafal study site) in Guinea Bissau. In Cafine-Cafal (Figure 5A), the planting area was 42.3%, while in Elalab (Figure 5B), it was 51.8% ($r^2 > 0.9$, p <0.001). The furrow area (Figure 2) varied between 48.2% and 57.7% between the two study sites when comparing the plots' area with the ridges' rice planting area.

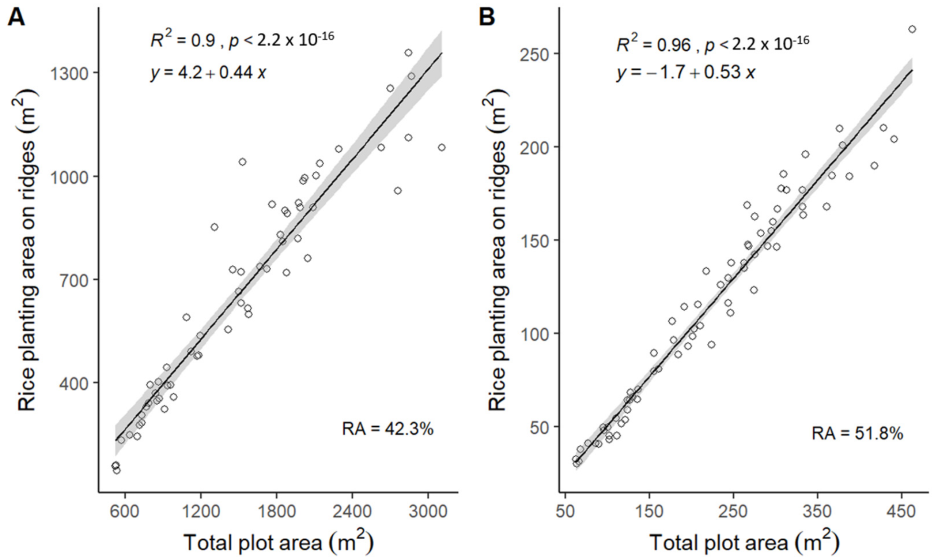

Figure 5. Effective rice-planting area on ridges (RA) evaluated in MSRPS plots in (**A**) Cafine-Cafal and (**B**) Elalab case study regions.

The number of rice production plots per hectare was seven times higher in the north than in the south of Guinea Bissau (Figure 6). The results showed that Elalab had approximately 53 plots per ha (10,000 m^2), while Cafine-Cafal had only about 7 plots per ha. When examining larger areas (>1 ha), there was high variability in the plots, as shown by the linear regressions ($r^2 = 0.72–0.75$, $p < 0.001$).

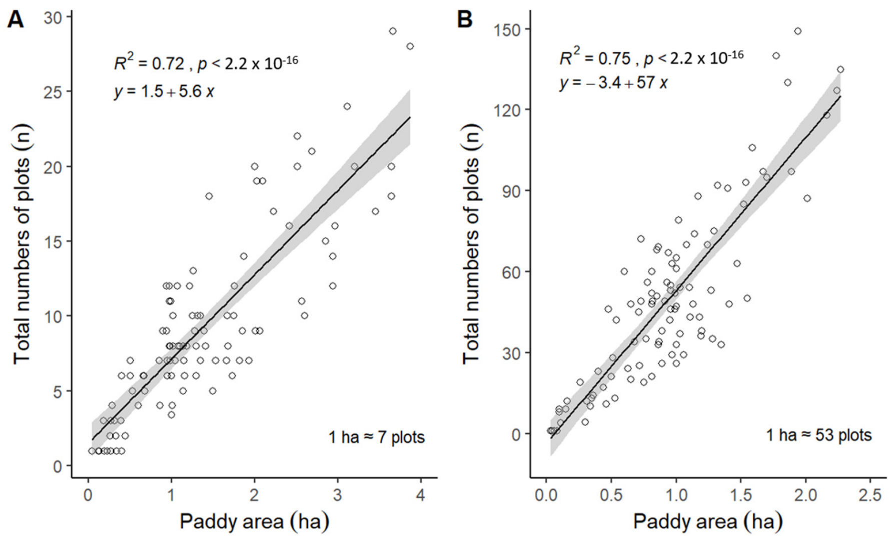

Figure 6. Estimation of the total numbers of plots per hectare in the MSRPSs of (**A**) Cafine-Cafal and (**B**) Elalab in Guinea Bissau.

3.4. Water-Harvesting Efficiency

As described in Section 2.2 (Experimental Observation and Data Collection), water depths were measured for nine points, as shown in Figure 3. Cafine-Cafal exhibited greater variation in waterlogging depths compared with Elalab (Figure 7), but the water depths in Elalab plots showed greater homogeneity. On average, a waterlogging depth of 37 cm was observed in Cafine-Cafal, while Elalab had a depth of 23 cm. The water-harvesting efficiencies (WL_{ef}) were 15 and 16% in Cafine-Cafal and Elalab. This approach quantified the hydrological effectiveness of a system by evaluating its water harvesting capacity relative to annual rainfall within the defined planting area of the plots. It is noteworthy that the recorded rainfall in the southern region during the 2021–2022 period amounted to 1411 mm in Elalab and 2426 mm in Cafine-Cafal (Figure 4). Thus, the water-harvesting efficiency was found to be similar due to the considerable number of plots in Elalab within one hectare.

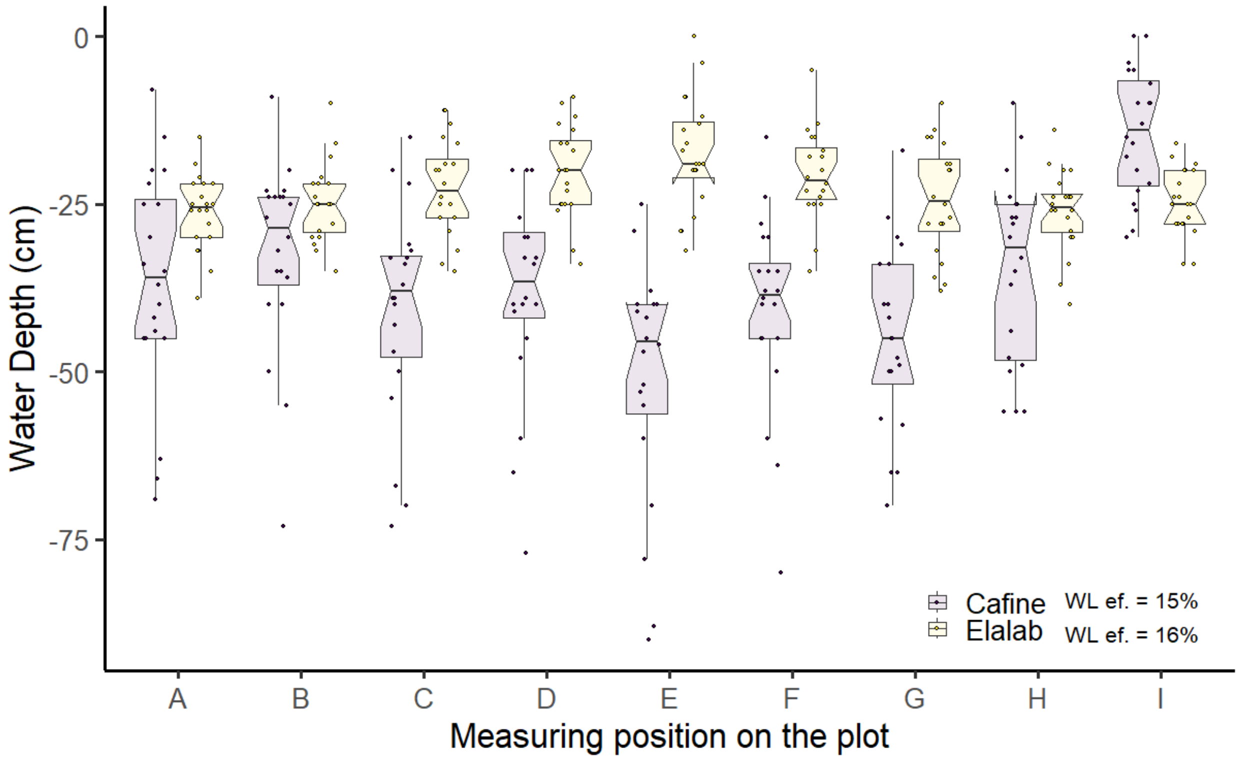

Figure 7. Variations in the waterlogging depth (August–September, peak rainfall) and water harvesting efficiency based on the total rainfall (WL_{ef}) in the 2021 and 2022 rainy seasons.

The water depth is a proxy for the topography of the plot floor. The bottom of the plots was more heterogeneous in the south of the country. Spatial analysis of the water levels in the southern plots revealed that the center had a shallower water depth (14.4 cm), while the edges had greater depths and water accumulations (<50.95 cm) (Figure 8A). Furthermore, water runoff showed a lateral distribution, with greater intensity in the corners of the plots. In contrast, in the Elalab study site, a more homogeneous distribution was found in the water level variation across the plots (Figure 8B). Thus, the water depth ranged between 17.6 cm and 26.6 cm and had a slope gradient directed toward one side of the plots.

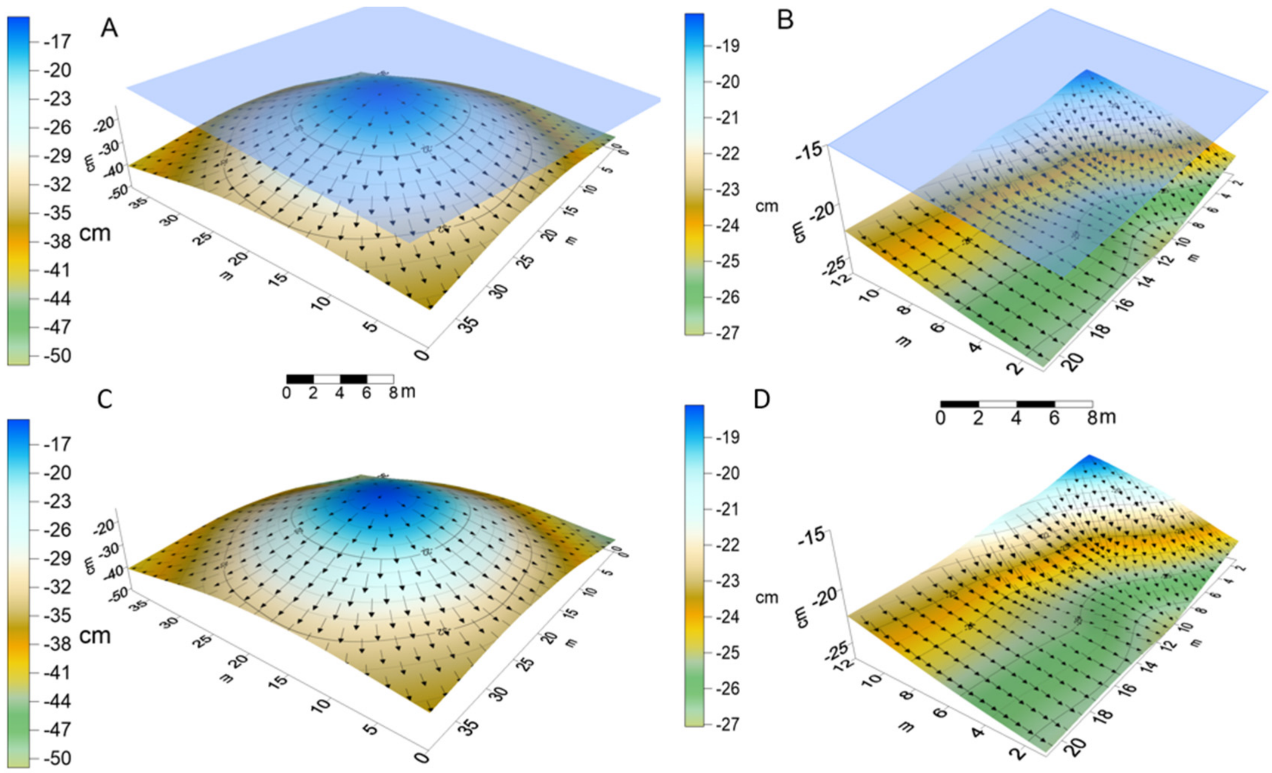

Figure 8. Radial basis function model used to estimate water level variation and water movement directions in the MSRPS plots in Guinea Bissau. Depth of the water (**A**) and slope gradient (**C**) in Cafine-Cafal. Depth of the water (**B**) and slope gradient (**D**) in Elalab.

3.5. Soil Consistency Limits

The soil consistency analysis shows that the plastic limit (PL) was higher for the southern study site than in the north. In Cafine-Cafal, PL corresponded to a gravimetric moisture content (θg) of 35.5% (Figure 9), which was statistically different ($p < 0.01$) from both the liquid limit (LL) (θg = 65.4%) and the sticky limit (SL) (θg = 29.8%). In Elalab, the PL was reached with a θg of 18.6%, and there was no statistical difference from the SL (θg = 16.7%). However, the LL showed a significant difference ($p < 0.01$) compared with the other limits (θg = 33.5%). The effort required for soil tillage in northern soils was likely significantly lower under conditions exhibiting less plasticity, as opposed to the plasticity condition observed in Cafine-Cafal.

Within the context of the spatial analysis, the consistency limits were found to be a regionalized variable, that is, they showed a pattern across a geographic area. This is shown by the geo-statistical interpolation parameters presented in Table 3. The geospatial correlation analysis demonstrated a global Moran's I index < 0, indicating spatial autocorrelation due to the high similarity of nearby points [75]. The variance in the consistency parameters was found to have a mean value of 0.002 in both study sites. The variance in Elalab showed a mean value ranging from 0.001 to 0.01. The clustering patterns were observed to be random (p = 0.01–<0.001). Therefore, interpolation indicates that they were related to spatial autocorrelation, which means they were random.

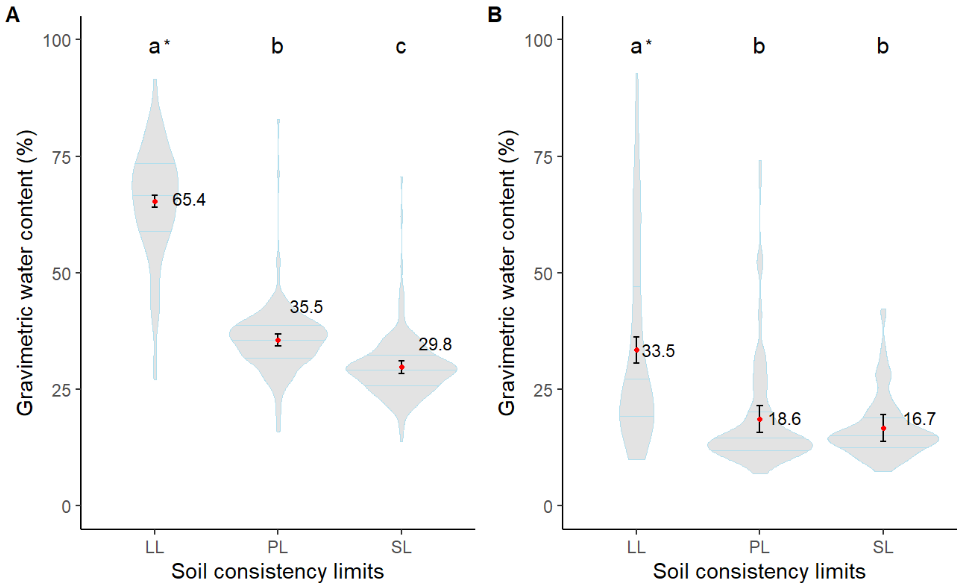

Figure 9. Soil consistency limits (including sticky limit [SL], plastic limit [PL], and liquid limit [LL]) in rice paddies for (**A**) Cafine-Cafal and (**B**) Elalab study sites in Guinea Bissau. * Mean values with the same letter did not differ significantly according to Tukey's test (α = 0.05).

Table 3. "Global Moran's I" evaluation and cross-validations calculated for soil consistency limits interpolation in Cafine-Cafal and Elalab in Guinea Bissau.

Samples	Global Moran's I	Variance	Z Punctuation	*p*-Value *	MAE	RMSE	P	MAE	RMSE	P	MAE	RMSE	P
	Cafine-Cafal Maps Interpolation				LOOCV			LOOCV—e_i			HM—e_i		
SL	0.182	0.002	3.964	<0.001	0.007	0.03	0.93	0.004	0.005	0.99	0.02	0.06	0.78
LL	0.159	0.0006	3.422	<0.001	0.02	0.04	0.94	0.01	0.02	0.99	0.05	0.08	0.76
PL	0.149	0.002	3.282	<0.001	0.02	0.04	0.90	0.01	0.02	0.98	0.04	0.07	0.73
	Elalab Maps Interpolation												
SL	0.22	0.002	4.502	<0.001	0.05	0.09	0.66	0.06	0.09	0.72	0.05	0.07	0.70
LL	0.115	0.003	2.333	0.01	0.10	0.14	0.75	0.09	0.13	0.80	0.10	0.13	0.79
PL	0.123	0.002	2.516	0.01	0.03	0.05	0.65	0.03	0.05	0.71	0.02	0.03	0.68

SL—sticky limit, LL—liquid limit, and PL—plastic limit. * A probability of less than 2% that the clustered pattern could be the result of a random likelihood. LOOCV—leave-one-out cross-validation. HM—holdout method (cross-validation). e_i—residual errors. RMSE—root-mean-square error. MAE—mean absolute error. P—Pearson's correlation coefficient.

The predictive ability of the interpolation was improved by subtracting residual errors "e_i" associated with previously interpolated values for each observation. It was found that after subtracting the residual errors, the LOOVC showed better parameter prediction (MAE and RMSE > 0.13) for each study site compared with the HM (Table 3). However, Elalab showed less accurate consistency limits prediction compared with Cafine-Cafal using the best predictive model. The average correlation between the observed and interpolated values showed that Cafine-Cafal had a rho (P) ranging from 98–99%, while Elalab showed a P between 71 and 80%. Therefore, a prediction model employed for the construction of a soil consistency map used LOOCV—e_i. This model could efficiently predict the specific locations or plots where farmers could identify the site for first plowing activities.

The geospatial distribution of soil consistency limits showed the sites with the highest plastic limit (PL) in the rice fields of Cafine-Cafal and Elalab (Figure 10). Paddies (Figure 2) exhibited a heterogeneous distribution in soil moisture contents, with a significantly lower PL found in the associated mangrove fields. The maximum PL was 57% in Cafine-Cafal and 28% in Elalab, suggesting that higher values of gravimetric moisture are suitable for manual soil preparation. The liquid limit (LL) range determined in Cafine-Cafal was between 35% and 86%, while in Elalab, these values ranged between 19% and 62%. The distribution of gravimetric moisture corresponding to each consistency limit on the maps shows the locations where the soil moisture suitable for plowing was reached more quickly.

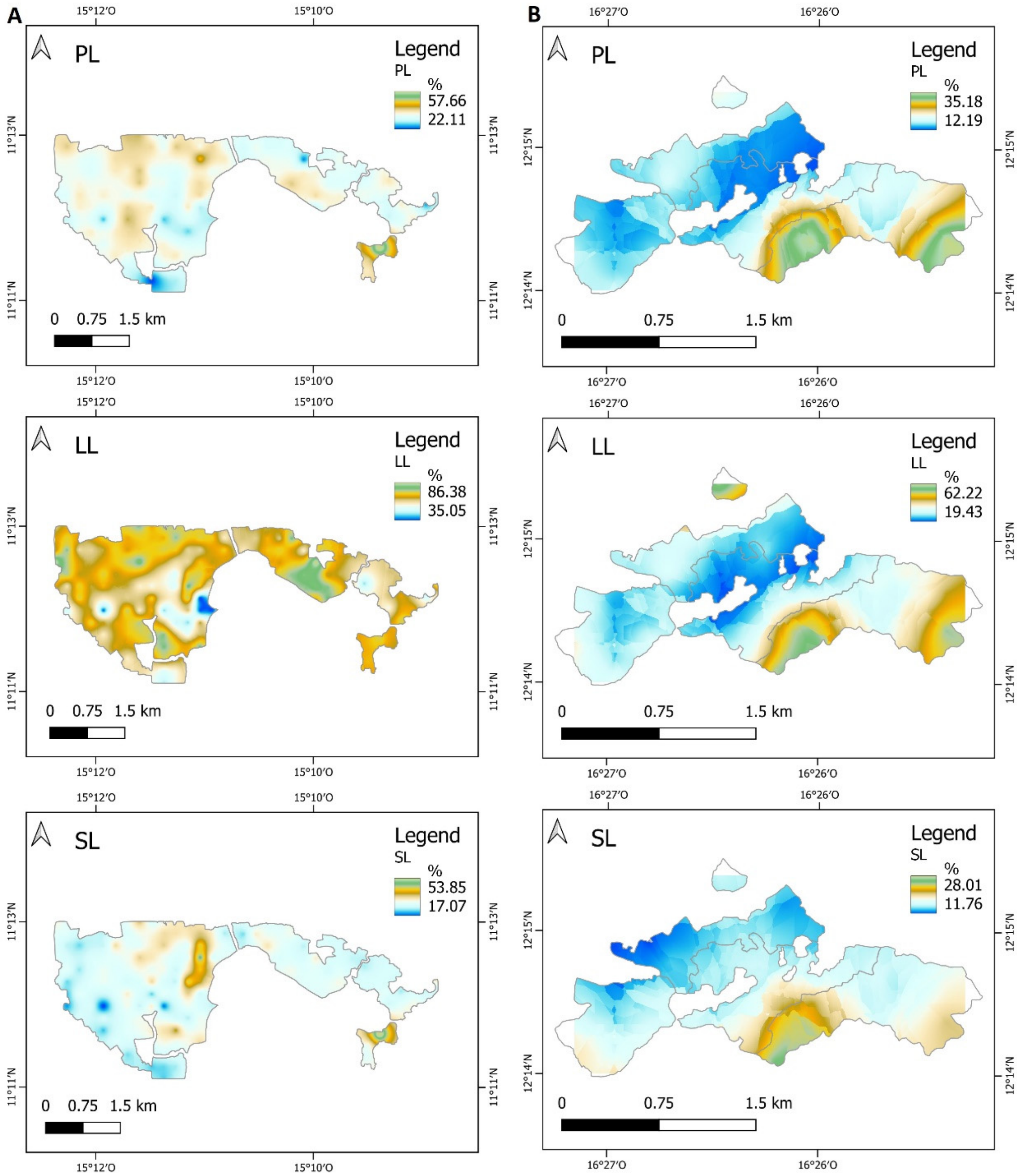

Figure 10. Interpolation of soil consistency limits, including the sticky limit (SL), plastic limit (PL), and liquid limit (LL), in MSRPSs of Cafine-Cafal (**A**) and Elalab (**B**), Guinea Bissau.

4. Discussion

The highly spatio-temporal variation in rainfall distribution (Figure 4) has a major impact on the MSRPS soil tillage calendar. While the total amount of rainfall (mm) has increased during recent decades, the rainy season often starts later and ends earlier, and there are many long dry spells. At the same time, rainfall is concentrated in fewer days, and heavy precipitations may occur, which can lead to flooding, dike breaches, brackish water entering the plots, and frequent harvest failures [20]. Thus, a high annual rainfall no longer guarantees a correspondingly high rice productivity. Until three decades ago, farmers used to sow the first nurseries between May and June, but today they have to wait until July or even August (Figure 4), depending on the location [26]. Then, the MSRPS depends on the amount of accumulated rainfall in the paddies and good water management [39,76]. Normally, soil tillage cannot begin until the paddies are sufficiently filled with rainwater (Figure 10) to leach or dissolve the salt, but according to soil consistency (Figure 9), it may not be necessary to wait until the plot is full of water. However, farmers drain the water (southern study site) in order to work the soil more easily and with less physical effort. However, the paddies must be filled with fresh water again so that rice can be transplanted or directly sown.

Rice production requires greater adaptability due to rainfall patterns in GB, and agricultural practices in the MSRPS need to be adapted to biophysical characteristics (Figure 10). Farmers usually start their cultivation on the plots given to them by their families (grandparents or parents) for soil preparation and have extensive practical knowledge of MRPS [77]. Many of these plots in both study sites (Figure 1) were located near the mangrove boundaries (tidal mangroves), where they require higher soil moisture due to a high Na^+ concentration (Table 2). Likewise, in many cases, these sites had a clay texture and required higher rainfall in order to overcome the plasticity limit, and thus, facilitate soil tillage. With changing rainfall patterns and a short rainy season window, farmers need to adapt and start tilling on plots that require less rainfall or soil moisture, such as plots with a loam or sand texture [78]. In this way, they can use these plots to plant nurseries and initiate the rice growth cycle since the species *Oryza glaberrima* and *O. sativa* require approximately 90 to 135 days from sowing to harvest [9,17,79–81]. This paper proposes an adaptation strategy that allows farmers to identify the sites where it is appropriate to initiate soil tillage (Figure 10). This will enable them to promote agriculture that is better adapted to rainfall patterns, which are likely to be more variable in the medium and long term. This is important for sustainable agriculture in GB given the climate variability [9].

The water management techniques used in Cafine-Cafal and Elalab differed (Figure 5), but both had similar water-harvesting efficiencies (Figure 7). When analyzing the Elalab study site ("Diola" and "Baiote" systems), it was clear that there was a much higher concentration of plots in a single hectare than in the southern study site of Cafine-Cafal ("Balanta") (Figure 6). The smaller paddies in the northern region (Elalab study site) allowed for better management of the scarce water supply. For example, the average rainfall in the 2021 and 2022 rainy seasons was 1454 mm in the Elalab study site and 2578 mm in Cafine-Cafal (Figure 4). These results are consistent with those of other researchers [20]. Although the plots may be larger in newly opened paddies, when Elalab farmers observed water accumulation in some areas, they divided them into two or more smaller plots (Figure 5). Smaller plots allowed for a more even distribution of water logging across the soil surface, both at the beginning and end of the rainy season (Figures 7 and 8). This meant that the desalinization of the paddies occurred more evenly and the amounts of water within the plots could be controlled more efficiently [18,19,26]. In contrast, Cafine-Cafal case study plots were seven times larger, and water management was less efficient despite the higher rainfall rates in the south of the country (Figure 6). This could lead to more heterogeneous runoff within plots, resulting in hot spots of salinization in the center of the paddies (Figure 8).

The efficiency in the use of production space was also higher in the north of Guinea Bissau than in the south. The Elalab case study achieved greater homogeneity of their ridges and furrows by using smaller plots (Figure 5) because the length of the ridges was shorter compared with those in the south ("Balantas"). On small plots, ridge dimensions can be better controlled when farmers till the soil. Since the ridges cover a larger area, farmers in the north could use four planting holes per row, while in the south, they used three holes in a triangle. This meant that northern farmers ("Diolas" and "Baiotes") were making better use of the area. In summary, the Elalab case study showed that the system had more efficient water management and labor use and was better adapted to water stress conditions. In the future, there is a possibility that the strategies implemented in the northern study sites will be effectively expanded to the southern regions and serve as an adaptive response to decreasing rainfall conditions.

Plastic limits (PLs) determine the time at which tillage can begin in the MSRPS fields (Figure 9). Currently, the agricultural calendar has a shorter time window, and gravimetric soil moisture (θg) is a tool that can be used to help define the appropriate moment and plots to start soil tillage each year. For this purpose, maps were modeled to determine the paddy areas where producers could start soil preparation (Table 3) to take advantage of the longest period of favorable conditions (high salt solubility) in the plots (Figure 10). It was found that the Cafine-Cafal farmers could start soil preparation with a θg = 36%, while in Elalab, approximately θg = 20% was required (Figure 9). These delineations provide farmers with valuable insights into the strategic management of soil friability and ensure avoiding soil sticking to the manual plows that are commonly used in MSRPS practices [9,12,17]. This is consistent with previous studies on soil workability and friability for agricultural production, which aim to help farmers make decisions on tillage operations [41,42,45,46,48]. Therefore, soil consistency is a tool to make soil management more efficient and achieve better water efficiency. However, it is the soil salinity that determines if it is possible to start planting or direct sowing immediately after plowing [19,26,35,40].

MSRPS infrastructures (bunds and dikes) are primarily designed for freshwater accumulation rather than salt removal or drainage. The vast majority of farmers only drain the water from the plots when they need to maintain a desired level of waterlogging according to the height of the rice plants. Nevertheless, farmers in the Elalab case study ("Diolas and Baiote") prioritized plowing the soil under waterlogging conditions to conserve the limited water availability (Figure 7). In addition to the additional physical effort required for soil preparation, this practice allowed the dissolved salts to remain in the water. This is in stark contrast with conventional irrigation systems, where many water management calculations are designed to facilitate salt leaching and removal, particularly in systems characterized by low rainfall but with greater availability of freshwater from wells or rivers. Therefore, MSRPS cultivation in both the northern and southern regions of Guinea Bissau presents complex variability in the biophysical characteristics of rice production areas, which pose major challenges.

5. Conclusions and Future Work

Rice production requires greater adaptability due to rainfall patterns in GB, and agricultural practices in the MSRPS need to be adapted to biophysical characteristics. The highly spatio-temporal variation in rainfall distribution has a major impact on the MSRPS soil tillage calendar. This paper proposes an adaptation strategy that allows farmers to identify the sites where they can initiate soil tillage. This will enable them to promote agriculture that is better adapted to rainfall patterns, which are likely to be more variable in the medium and long term. This is important for sustainable agriculture in GB given climate variability.

It could be concluded that the water management techniques used in the north and the south of the country differed, but both had similar water-harvesting efficiencies. The smaller paddies in the northern region (Elalab study site) allow for better management of the scarce water supply. Smaller plots allow for a more even distribution of water depths across the soil surface, both at the beginning and end of the rainy season. This means that the desalinization of the paddies occurred more evenly and the amounts of water within the plots can be controlled more efficiently. In contrast, in the south, plots were seven times larger, and water management was less efficient despite the higher rainfall rates, which could lead to more heterogeneous runoff within plots, resulting in hot spots of salinization in the center of the paddies.

Currently, the agricultural calendar has a shorter time window and gravimetric soil moisture (θg) is proposed as a tool to help determine the appropriate time and sites to start tillage each year. Soil consistency maps were modeled to determine the plots where producers could begin soil preparation to take advantage of the longest period of favorable conditions (high salt solubility) in the plots. These delineations provide farmers with valuable insights into the strategic management of soil friability and ensure avoiding soil sticking to the plows that are commonly used in MSRPS practices.

The comparative study of some biophysical properties between study sites facilitated the identification of specific constraints hindering rice growth and productivity due to salinity and water management. The key limitations identified that will guide our future research were as follows: (i) The lack of an effective drainage system in the plots resulted in the productivity of the plots relying solely on leaching and salt dissolution. (ii) Irregularities in the topography of the plots could lead to a heterogeneous accumulation of salts, leading to significant variability in rice production. (iii) Inadequate knowledge of the chemical composition of salts and the physical properties of soil hindered the ability to effectively address challenges related to managing soil alkalinity, toxicity, and acidity. The MSRPS lacked maps that provide information on initial salinity conditions, and the development of such resources could greatly improve decision-making processes, particularly during periods of low rainfall. (iv) There is no water-balance data on the MSRPS allowing for the determination of the optimal conditions for rice growth in both the initial and final growth stages.

Author Contributions: Conceptualization, G.G., P.P. and M.d.R.C.; methodology, G.G.; software, G.G. and J.C.; validation, M.T., M.d.R.C. and P.P.; formal analysis, G.G. and J.C.; investigation, G.G. and J.S.; resources, M.T.; data curation, G.G.; writing—original draft preparation, G.G.; writing—review and editing, M.d.R.C., P.P., J.S. and M.T.; visualization, G.G. and J.C.; supervision, M.d.R.C., P.P. and M.T.; project administration, M.T.; funding acquisition, M.T. All authors have read and agreed to the published version of the manuscript.

Funding: This research article was made possible thanks to the financial support provided by the European Union through the DeSIRA project Titled "Mangroves, Mangrove Rice and Mangrove People: Sustainably Improving Rice Production, Ecosystem, and Livelihoods (grant contract FOOD/2019/412-700) (https://www.malmon-desira.com, accessed on 28 December 2023).

Data Availability Statement: Data will be provided upon request.

Acknowledgments: The support of the Fundaçao para a Ciência e a Tecnologia, Portugal, through the grant attributed to the research unit Forest Research Centre (CEF) UIDB/00239/2020, as well as in the research unit LEAF—Linking Landscape, Environment, Agriculture and Food Research Centre (UIDB/04129/2020) of the TERRA associated laboratory. Additionally, this research received support from the University of Costa Rica. The authors extend their gratitude to Viriato Cossa, Merlin Leunda-Martiarena, Filipa Zacarias, Paulina Na-Bitchom, Eduino Mendes da Costa, Nelson Seidi, Adriano Barbosa, Alqueia Intchama, and Adinane Jalo for their invaluable support, insightful suggestions, meticulous sample collection, laboratory analyses, and dedicated work in the study sites of Guinea Bissau.

Conflicts of Interest: The authors declare no conflicts of interest.

References

1. Food and Agriculture Organization of the United Nations FAO Rice Market Monitor. Available online: https://www.fao.org/markets-and-trade/commodities/rice/rmm/en/ (accessed on 28 December 2023).
2. Kraehmer, H.; Thomas, C.; Vidotto, F. Rice Production in Europe. In *Rice Production Worldwide*; Springer International Publishing: Cham, Switzerland, 2017; pp. 93–116, ISBN 9783319475165.
3. Chauhan, B.S.; Jabran, K.; Mahajan, G. (Eds.) *Rice Production Worldwide*; Springer International Publishing: Cham, Switzerland, 2017; ISBN 978-3-319-47514-1.
4. Kyle, S. *Working Paper Rice Sector Policy Options in Guinea Bissau*; Department of Applied Economics and Management, Cornell University: New York, NY, USA, 2015.
5. Ukpong, I.E. An Ordination Study of Mangrove Swamp Communities in West Africa. *Vegetatio* **1995**, *116*, 147–159. [CrossRef]
6. García del Toro, E.M.; Más-López, M.I. Changes in Land Cover in Cacheu River Mangroves Natural Park, Guinea-Bissau: The Need for a More Sustainable Management. *Sustainability* **2019**, *11*, 6247. [CrossRef]
7. Temudo, M.P.; Cabral, A.I. The Social Dynamics of Mangrove Forests in Guinea-Bissau, West Africa. *Hum. Ecol.* **2017**, *45*, 307–320. [CrossRef]

8. Hawthorne, W. Nourishing a Stateless Society during the Slave Trade: The Rise of Balanta Paddy-Rice Production in Guinea-Bissau. *J. Afr. Hist.* **2001**, *42*, 1–24. [CrossRef] [PubMed]
9. Temudo, M.P. Planting Knowledge, Harvesting Agro-Biodiversity: A Case Study of Southern Guinea-Bissau Rice Farming. *Hum. Ecol.* **2011**, *39*, 309–321. [CrossRef]
10. Linares, O.F. From Tidal Swamp to Inland Valley: On the Social Organization of Wet Rice Cultivation among the Diola of Senegal. *Africa* **1981**, *51*, 557–595. [CrossRef]
11. Martiarena, M.L.; Temudo, M.P. Endogenous Learning and Innovation in African Smallholder Agriculture: Lessons from Guinea-Bissau. *J. Agric. Educ. Ext.* **2023**, 1–19. [CrossRef]
12. Temudo, M.P. Men Wielding the Plough: Changing Patterns of Production and Reproduction among the Balanta of Guinea-Bissau. *J. Agrar. Chang.* **2018**, *18*, 267–280. [CrossRef]
13. Van Ghent, P.A.M.; Ukkerman, R. *The Balanta Rice Farming System in Guinea Bissau*; WUR: Wageningen, The Netherlands, 1993.
14. Écoutin, J.-M.; Barry, M.; Bouiu, S.; Charles-Dominique, E.; Journet, O.; Penot, E.; Ruë, O.; Souaré, D.; Sow, M. Aménagement Technique Du Milieu. In *Rivières du Sud: Societes et Mangroves Ouestafricaines*; Cormier-Salem, M.C., Ed.; IRD: Paris, France, 1999; pp. 209–268.
15. Espírito-Santo, J. Notas Sobre a Cultura do Arroz Entre os Balantas. *Bol. Cult. Guiné Port.* **1949**, *4*, 197–232.
16. Schwarz, C. Os Ecossistemas Orizícolas da Guiné–Bissau. *Comunicações* **1993**, *13*, 367–388.
17. Tesio, F.; Camerini, F.; Maucieri, G.; Bertini, C.; Cerise, S. Mangrove Rice Biodiversity Valorization in Guinea Bissau. A Bottom-up Approach. *Exp. Agric.* **2021**, *57*, 244–254. [CrossRef]
18. van Oort, P.A.J. Mapping Abiotic Stresses for Rice in Africa: Drought, Cold, Iron Toxicity, Salinity and Sodicity. *Field Crop. Res.* **2018**, *219*, 55–75. [CrossRef]
19. Baggie, I.; Sumah, F.; Zwart, S.J.; Sawyerr, P.; Bandabla, T.; Kamara, C.S. Characterization of the Mangrove Swamp Rice Soils along the Great Scarcies River in Sierra Leone Using Principal Component Analysis. *Catena* **2018**, *163*, 54–62. [CrossRef]
20. Mendes, O.; Fragoso, M. Assessment of the Record-Breaking 2020 Rainfall in Guinea-Bissau and Impacts of Associated Floods. *Geosciences* **2023**, *13*, 25. [CrossRef]
21. Davidson, J. "We Work Hard": Customary Imperatives of the Diola Work Regime in the Context of Environmental and Economic Change. *Afr. Stud. Rev.* **2009**, *52*, 119–141. [CrossRef]
22. Andrieu, J. Land Cover Changes on the West-African Coastline from the Saloum Delta (Senegal) to Rio Geba (Guinea-Bissau) between 1979 and 2015. *Eur. J. Remote Sens.* **2018**, *51*, 314–325. [CrossRef]
23. Temudo, M.P.; Cabral, A.I.R. Climate Change as the Last Trigger in a Long-Lasting Conflict: The Production of Vulnerability in Northern Guinea-Bissau, West Africa. *J. Peasant Stud.* **2023**, *50*, 315–338. [CrossRef]
24. Raimundo Lopes, N.D.; Li, T.; Qian, D.; Matomela, N.; Sá, R.M. Factors Influencing Coastal Land Cover Change and Corresponding Impact on Habitat Quality in the North-Western Coastline of Guinea-Bissau (NC-GB). *Ocean Coast. Manag.* **2022**, *224*, 106181. [CrossRef]
25. Thiam, S.; Villamor, G.B.; Kyei-Baffour, N.; Matty, F. Soil Salinity Assessment and Coping Strategies in the Coastal Agricultural Landscape in Djilor District, Senegal. *Land Use Policy* **2019**, *88*, 104191. [CrossRef]
26. Dossou-Yovo, E.R.; Devkota, K.P.; Akpoti, K.; Danvi, A.; Duku, C.; Zwart, S.J. Thirty Years of Water Management Research for Rice in Sub-Saharan Africa: Achievement and Perspectives. *Field Crop. Res.* **2022**, *283*, 108548. [CrossRef]
27. Andreetta, A.; Huertas, A.D.; Lotti, M.; Cerise, S. Land Use Changes Affecting Soil Organic Carbon Storage along a Mangrove Swamp Rice Chronosequence in the Cacheu and Oio Regions (Northern Guinea-Bissau). *Agric. Ecosyst. Environ.* **2016**, *216*, 314–321. [CrossRef]
28. Dexter, A.; Bird, N.R. Methods for Predicting the Optimum and the Range of Soil Water Contents for Tillage Based on the Water Retention Curve. *Soil Tillage Res.* **2001**, *57*, 203–212. [CrossRef]
29. Penot, E. La Riziculture de Mangrove Balante de la Region de Tombali En Guinée-Bissau, Ou l'adaptation d'une Société Rizicole Africaine Traditionnelle à Travers Un Siècle de Changements Majeurs. In Proceedings of the Séminaire Rizic. en Afrique l'Ouest, Bordeaux, France, 5–7 April 1995; p. 19.
30. Garbanzo, G.; Cameira, R.; Temudo, M.; Paredes, P. Mangrove Swamp Rice Production System of Guinea Bissau: Identification of Main Constraints Associated with Salinity and Rainfall Variability. *Agronomy* 2024, *submitted*.
31. Nambiar, K.K.; Gupta, A.; Fu, Q.; Li, S. Biophysical, Chemical and Socio-Economic Indicators for Assessing Agricultural Sustainability in the Chinese Coastal Zone. *Agric. Ecosyst. Environ.* **2001**, *87*, 209–214. [CrossRef]
32. Martínez-López, J.; Bertzky, B.; Willcock, S.; Robuchon, M.; Almagro, M.; Delli, G.; Dubois, G. Remote Sensing Methods for the Biophysical Characterization of Protected Areas Globally: Challenges and Opportunities. *ISPRS Int. J. Geo-Inf.* **2021**, *10*, 384. [CrossRef]
33. Fang, H.; Liang, S.; McClaran, M.P.; van Leeuwen, W.J.D.; Drake, S.; Marsh, S.E.; Thomson, A.M.; Izaurralde, R.C.; Rosenberg, N.J. Biophysical Characterization and Management Effects on Semiarid Rangeland Observed from Landsat ETM+ Data. *IEEE Trans. Geosci. Remote Sens.* **2005**, *43*, 125–134. [CrossRef]
34. Singh, M.; Kalra, N.; Chakraborty, D.; Kamble, K.; Barman, D.; Saha, S.; Mittal, R.B.; Pandey, S. Biophysical and Socioeconomic Characterization of a Water-Stressed Area and Simulating Agri-Production Estimates and Land Use Planning under Normal and Extreme Climatic Events: A Case Study. *Environ. Monit. Assess.* **2008**, *142*, 97–108. [CrossRef]

35. Bos, D.; Grigoras, I.; Ndiaye, A. *Land Cover and Avian Biodiversity in Rice Fields and Mangroves of West Africa*; A&W-Report; Wetlands International: Dakar, Senegal, 2006; ISBN 9789058820341.
36. Ukpong, I.E. Vegetation and Its Relation to Soil Nutrient and Salinity in the Calabar Mangrove Swamp, Nigeria. *Mangroves Salt Marshes* **1997**, *1*, 211–218. [CrossRef]
37. Temudo, M.P.; Cabral, A.I.R.; Reis, P. The Sea Swallowed Our Houses and Rice Fields: The Vulnerability to Climate Change of Coastal People in Guinea-Bissau, West Africa. *Hum. Ecol.* **2022**, *50*, 835–850. [CrossRef]
38. Merkohasanaj, M.; Cortez, N.; Goulao, L.; Andreetta, A. Characterisation of Physical-Chemical and Fertility Dynamics of Mangrove Soils from Guinea-Bissau in Different Agroecological Conditions Underlying Paddy Rice Cultivation Ao Cultivo Do Arroz. *Rev. Cienc. Agrar.* **2022**, *45*, 267–271. [CrossRef]
39. Fandé, M.B.; Ponte Lira, C.; Penha-Lopes, G. Using TanDEM-X Global DEM to Map Coastal Flooding Exposure under Sea-Level Rise: Application to Guinea-Bissau. *ISPRS Int. J. Geo-Inf.* **2022**, *11*, 225. [CrossRef]
40. Sylla, M.; Stein, A.; van Breemen, N.; Fresco, L.O. Spatial Variability of Soil Salinity at Different Scales in the Mangrove Rice Agro-Ecosystem in West Africa. *Agric. Ecosyst. Environ.* **1995**, *54*, 1–15. [CrossRef]
41. Utomo, W.H.; Dexter, A.R. Soil Friability. *J. Soil Sci.* **1981**, *32*, 203–213. [CrossRef]
42. Obour, P.B.; Lamandé, M.; Edwards, G.; Sørensen, C.G.; Munkholm, L.J. Predicting Soil Workability and Fragmentation in Tillage: A Review. *Soil Use Manag.* **2017**, *33*, 288–298. [CrossRef]
43. Cresswell, H.P.; Painter, D.J.; Cameron, K.C. Tillage and Water Content Effects on Surface Soil Physical Properties. *Soil Tillage Res.* **1991**, *21*, 67–83. [CrossRef]
44. Sharma, B.; Bora, P.K. Plastic Limit, Liquid Limit and Undrained Shear Strength of Soil—Reappraisal. *J. Geotech. Geoenviron. Eng.* **2003**, *129*, 774–777. [CrossRef]
45. Arvidsson, J.; Bölenius, E. Effects of Soil Water Content during Primary Tillage—Laser Measurements of Soil Surface Changes. *Soil Tillage Res.* **2006**, *90*, 222–229. [CrossRef]
46. Keller, T.; Dexter, A.R. Plastic Limits of Agricultural Soils as Functions of Soil Texture and Organic Matter Content. *Soil Res.* **2012**, *50*, 7. [CrossRef]
47. Boekel, P.; Peerlkamp, P.L. Soil Consistency as a Factor Determining the Soil Structure of Clay Soils. *Neth. J. Agric. Sci.* **1956**, *4*, 122–125. [CrossRef]
48. Keller, T.; Arvidsson, J.; Dexter, A. Soil Structures Produced by Tillage as Affected by Soil Water Content and the Physical Quality of Soil. *Soil Tillage Res.* **2007**, *92*, 45–52. [CrossRef]
49. Haigh, S.K.; Vardanega, P.J.; Bolton, M.D. The Plastic Limit of Clays. *Géotechnique* **2013**, *63*, 435–440. [CrossRef]
50. Beck, H.E.; Zimmermann, N.E.; McVicar, T.R.; Vergopolan, N.; Berg, A.; Wood, E.F. Present and Future Köppen-Geiger Climate Classification Maps at 1-Km Resolution. *Sci. Data* **2018**, *5*, 180214. [CrossRef]
51. Sambú, F.B. Variabilidade Climática da Precipitação na Região da Guiné-Bissau: Situação Sinóptica e a Influencia dos Sistemas Convectivos. Master's Thesis, Universidade de Évora, Évora, Portugal, 2003.
52. Balasubramanian, V.; Sie, M.; Hijmans, R.J.; Otsuka, K. Increasing Rice Production in Sub-Saharan Africa: Challenges and Opportunities. *Adv. Agron.* **2007**, *94*, 55–133. [CrossRef]
53. Teixeira, D.S. *Os Solos Da Guiné Portuguesa. Carta General Caracteristicas, Formação e Utilização*, 1st ed.; Junta de Investigações do Ultramar: Lisboa, Portugal, 1962.
54. Schoeneberger, P.; Wysocki, E.C.B.; Staff, S.S. *Field Book for Describing and Sampling Soils*; Version 3.0; Natural Resources Conservation Service, National Soil Survey Center: Lincoln, NE, USA, 2012; Volume 258.
55. Soil Survey Staff. *Keys to Soil Taxonomy*, 13th ed.; USDA, Ed.; Natural Resourses Conservation Service: Lincoln, NE, USA, 2022.
56. Sylla, M. Soil Salinity and Acidity: Spatial Variabily and Effects on Rice Production in West Africa's Mangrove Zone. Ph.D. Thesis, Wageningen University and Research, Wageningen, The Netherlands, 1994.
57. Marius, C.; Lucas, J. Holocene Mangrove Swamps of West Africa Sedimentology and Soils. *J. Afr. Earth Sci.* **1991**, *12*, 41–54. [CrossRef]
58. Casagrande, A. Notes on the Design of the Liquid Limit Device. *Géotechnique* **1958**, *8*, 84–91. [CrossRef]
59. Sowers, G. *Methods of Soil Analysis*; Black, C.A., Ed.; Agronomy Monographs; American Society of Agronomy, Soil Science Society of America: Madison, WI, USA, 1965; ISBN 9780891182030.
60. *ASTM D4318-17*; Standard Test Methods for Liquid Limit, Plastic Limit, and Plasticity Index of Soils. ASTM International: West Conshohocken, PA, USA, 2010.
61. O'Kelly, B.C.; Vardanega, P.J.; Haigh, S.K. Use of Fall Cones to Determine Atterberg Limits: A Review. *Géotechnique* **2018**, *68*, 843–856. [CrossRef]
62. Sivakumar, V.; O'Kelly, B.C.; Henderson, L.; Moorhead, C.; Chow, S.H. Measuring the Plastic Limit of Fine Soils: An Experimental Study. *Proc. Inst. Civ. Eng.-Geotech. Eng.* **2015**, *168*, 53–64. [CrossRef]
63. Soil Survey Staff. *Kellogg Soil Survey Laboratory Methods Manual*; Version 6; Natural Resourses Conservation Service: Lincoln, NE, USA, 2022.
64. Posit Team RStudio: Integrated Development Environment for R. Available online: http://www.posit.co/ (accessed on 28 December 2023).
65. Poggio, L.; Gimona, A. 3D Mapping of Soil Texture in Scotland. *Geoderma Reg.* **2017**, *9*, 5–16. [CrossRef]

66. Mosleh, Z.; Salehi, M.H.; Jafari, A.; Borujeni, I.E.; Mehnatkesh, A. The Effectiveness of Digital Soil Mapping to Predict Soil Properties over Low-Relief Areas. *Environ. Monit. Assess.* **2016**, *188*, 195. [CrossRef] [PubMed]
67. Adhikari, K.; Kheir, R.B.; Greve, M.B.; Bøcher, P.K.; Malone, B.P.; Minasny, B.; McBratney, A.B.; Greve, M.H. High-Resolution 3-D Mapping of Soil Texture in Denmark. *Soil Sci. Soc. Am. J.* **2013**, *77*, 860–876. [CrossRef]
68. Zeraatpisheh, M.; Ayoubi, S.; Mirbagheri, Z.; Mosaddeghi, M.R.; Xu, M. Spatial Prediction of Soil Aggregate Stability and Soil Organic Carbon in Aggregate Fractions Using Machine Learning Algorithms and Environmental Variables. *Geoderma Reg.* **2021**, *27*, e00440. [CrossRef]
69. Garbanzo-León, J.G.; Alemán-Montes, B.; Alvarado-Hernández, A.; Henríquez-Henríquez, C. Validación de Modelos Geoestadísticos y Convencionales en la Determinación de la Variación Espacial de la Fertilidad de Suelos del Pacífico sur de Costa Rica. *Investig. Geogr.* **2017**, *2017*, 20–41. [CrossRef]
70. Kunhikrishnan, A.; Thangarajan, R.; Bolan, N.S.; Xu, Y.; Mandal, S.; Gleeson, D.B.; Seshadri, B.; Zaman, M.; Barton, L.; Tang, C.; et al. Functional Relationships of Soil Acidification, Liming, and Greenhouse Gas Flux. In *Advances in Agronomy*; Academic Press: London, UK, 2016; Volume 139, pp. 1–71, ISBN 9780128047736.
71. Espinosa, J.; Molina, E. *Acidez y Encalado de los Suelos*, 1st ed.; International Plan Nutrition Institute: Peachtree Corners, GA, USA, 1999; ISBN 2013206534.
72. Grattan, S.R.; Grieve, C.M. Mineral Element Acquisition and Growth Response of Plants Grown in Saline Environments. *Agric. Ecosyst. Environ.* **1992**, *38*, 275–300. [CrossRef]
73. Kirkby, E.A.; Nikolic, M.; White, P.J.; Xu, G. Mineral Nutrition, Yield, and Source–Sink Relationships. In *Marschner's Mineral Nutrition of Plants*; Elsevier: Amsterdam, The Netherlands, 2023; pp. 131–200, ISBN 9780128197738.
74. Chapman, H.D. Cation-Exchange Capacity. In *Methods of Soil Analysis, Part 2: Chemical and Microbiological Properties*; American Society of Agronomy, Inc.: Madison, WI, USA, 2016; pp. 891–901, ISBN 9780891182047.
75. Chen, Y. New Approaches for Calculating Moran's Index of Spatial Autocorrelation. *PLoS ONE* **2013**, *8*, e68336. [CrossRef]
76. Santos, C.; Mourato, J.M. 'I Was Born Here, I Will Die Here': Climate Change and Migration Decisions from Coastal and Insular Guinea-Bissau. *Geogr. Ann. Ser. B Hum. Geogr.* **2022**, 1–19. [CrossRef]
77. Temudo, M.P. Inovação e Mudança Em Sociedades Rurais Africanas Gestão de Recursos Naturais, Saber Local e Instituições de Desenvolvimento Induzido Estudo de Caso Na Guiné-Bissau. Ph.D. Thesis, Universidade Técnica de Lisboa, Lisbon, Portugal, 1998.
78. Unger, P. *Soil Tillage in Africa: Needs and Challenges. Land and Water Development Division*; Food and Agriculture Organization of the United Nations: Roma, Italy, 1984; ISBN 9251034427.
79. Linares, O.F. African Rice (*Oryza glaberrima*): History and Future Potential. *Proc. Natl. Acad. Sci. USA* **2002**, *99*, 16360–16365. [CrossRef] [PubMed]
80. Miranda, I. Pesquisa Orizícola Guineense. *Comun. Intituto Invesigacion Científica Trop.* **1993**, 97–114.
81. Penot, E. L'économie d'une Société Rizicole Traditionnelle En Pleine Mutation: La Société Balante de la Région de Tombali En Guinée Bissau. 1992. Available online: https://agritrop.cirad.fr/577623/ (accessed on 28 December 2023).